AJG

Article

Vegetation Growth Abnormality by NDVI's Response to Precipitation in Mongolia with Emphasis on Its Grassland through LULC from 2001 to 2020

Guanyu YAN* and Wataru TAKEUCHI

Bw-605, W. Takeuchi Lab, Institute of Industrial Science, the University of Tokyo

4-6-1 Komaba, Meguro-Ku, Tokyo, 153-8505, Japan

*Corresponding author: G. YAN <guanyu@g.ecc.u-tokyo.ac.jp>

Received: August 26, 202; Accepted: December 23, 2022; Published: December 30, 2022

Abstract

The sustainability of the natural environment is vital to Mongolia due to pastoralism. It is easy to observe the phenology of vegetation growth represented by NDVI but challenging to tell vegetation changes due to human interventions from rainfall fluctuations. This can be solved through NDVI's response to precipitation changes. We calculated the temporal Pearson Correlation Value between NDVI and Precipitation data in Mongolia from 2001 to 2020, emphasizing grassland changes with MODIS LULC. In this period, the mean and median values of NDVI-Precipitation Correlation Values are 0.327 and 0.331, with a standard deviation of 0.204. Grassland has grown 4.69%, and about 51% of grassland is deemed abnormal in vegetation growth by the NDVI-Precipitation correlation. There are substantial portions of grassland in Mongolia under heavy stress, although the overall NDVI of grassland is increasing. Model verification shows NDVI-Precipitation Correlation Value = 0.330-0.008 × Population Density, which links low correlation value to higher population density.

Keywords: NDVI, GSMaP, Pearson Correlation, Time series data, Arid lands, Biomass

1. Introduction

1.1 Background

Pastures make up almost 95 percent of Mongolian agricultural land, among which about 70 percent have degraded ("Mongolia at a Glance," FAO). Understanding the scale and distribution of abnormality in vegetation growth is vital in protecting the local environment. Due to climate change, natural hazards, and overgrazing, there have been reports of increasing grassland degradation, which puts severe risks to the livelihood of many people in Mongolia (Liu et al., 2013; Densambuu et al., 2018). And on the background of climate change, the general climate trends in Mongolia could be shifting into new patterns (Angerer et al., 2008). Entering the 21st century, almost a decade after the downfall of the

USSR, Mongolia has been transformed into a market economy. The nomadic groups conducting animal husbandry rely more heavily on raising cashmere-producing goats, further contributing to the overgrazing problem (Maekawa 2013). According to Mongolia's National Statistical Office, the number of livestock has increased 2.6 times from 2001 to 2020 ("Livestock," NSO of Mongolia). The accompanied water-soil erosion problems like sandstorms are not only a regional issue but also an international concern (Natsagdorj et al., 2003; Shao et al., 2006; Zhang et al., 2008). Since the social-economic reform in the 1990s, Mongolian society has been relatively stable for 20 years, giving us a suitable time window to observe the changes in the natural environment.

As a vast country of around 1.6 million Square Kilometers, Mongolia only harbors a population of 3.35 million people. And only 30% of the total population lives in rural areas conducting animal husbandry ("POPULATION OF MONGOLIA," NSO of Mongolia). It is challenging to run a national-scale on-site investigation with such a low population density where observation conducted on satellite platforms in Remote Sensing could be of great strength and assistance. Researchers working with Remote Sensing datasets pointed out that vegetation and climatic factors work directly and indirectly, and precipitation is one of the critical factors we need to consider (Dale et al., 2000).

To represent vegetation growth in the Remote Sensing dataset, we use the Normalized Difference Vegetation Index (NDVI) to monitor vegetation growth status and phenology patterns (Carlson and Ripley, 1997; Zhao et al., 2011; Pettorelli et al., 2005). Some researchers investigated the long-term NDVI dynamics and responses to climatic change in the Mongolian plateau and found out the most common growth period for vegetation is from April to October (Bao et al., 2014). And in dealing with yearly records, other researchers claim that the annual maximum NDVI value can represent that year's growth. At the same time, precipitation during the growing season can be utilized as the response amount of rainfall (Ding et al., 2007). Mongolia and Inner Mongolia divide the Mongolian Plateau. For the Southern part, people concluded that general restoration is observable even though human activity is still the first reason for grassland degradation (Zhang et al., 2020). To preserve the future sustainability of the local environment, we need to investigate and observe the human factor's impact on vegetation growth on a national level. And a retrospective checkup of existing records helps us better prepare for the future (Mirza 2003; Stott 2016).

Usually, with the increase in

precipitation, vegetation growth would also increase. However, in the case of Mongolia, the amount of vegetation growth we can observe could be what is left of grazing activities that might not be in good correlation with precipitation, and the acquired spatial-temporal change patterns of NDVI, therefore, contain bias caused by third-party influences. Should we only focus on the decrease in vegetation growth, we would introduce the bias by ignoring patches that have a growing amount of vegetation coverage but suffer more from grazing. Researchers also mentioned that in some of their research sites, high pasture load caused a digression of vegetation (Tulokhonov et al., 2014). And because of this, some researchers criticized the applicability of widely used correlation and regression analysis, stressing their inflexibility as linear statistical models could not accurately describe the relationships between the NDVI and Precipitation (Meng et al., 2020). However, the authors believe this "poor correlation" is a good indicator of the levels of impact of human activities. In primarily arid and semi-arid Mongolia (Beck et al., 2018), the correlation coefficient would be a high positive number between NDVI and precipitation under ideal conditions. So, places with low or negative correlations could be under heavy grazing stress or other anthropogenic influences. Thus, our calculation can count in all kinds of negative impacts, even in places with an increasing trend of vegetation coverage.

1.2 Novelty and Objectives

This work distinguishes itself in its broad scale, both temporally and spatially. It spans over two decades of data till the year 2020. It covers the whole of Mongolia, making the research more representative than research that uses data only from a brief time and partial regions of Mongolia (Sekiyama et al., 2015; Jargalsaikhan, 2013; Nanzad et al., 2019; Nyamsuren et al., 2019). Our unique interpretation and implementation of correlation analysis provide a simple yet powerful way of understanding the environmental time-series data in arid and semi-arid climates and producing a geospatial distribution of biomass fluctuation by climatic factors and human intervention.

This paper aims to observe the characteristics of the correlation between vegetation growth represented by NDVI and precipitation change in Mongolia annually between 2001 and 2020 and to use the correlation analysis result of the NDVI-Precipitation pair to evaluate grassland fluctuations in Mongolia in the first two decades of the 21st Century.

2. Material & Method

The general workflow of this paper (figure 2.1) is that NDVI and Precipitation Data produced the temporal

Pearson correlation results as the vegetation growth abnormality index. After data exploration and discussion of the outcome, MODIS LULC data was introduced to make grassland change rates, biomass density, impacted area changes, average precipitation, and rainfall utilities from 2001 to 2020 in Mongolia. We finished our work with a verification discussion.

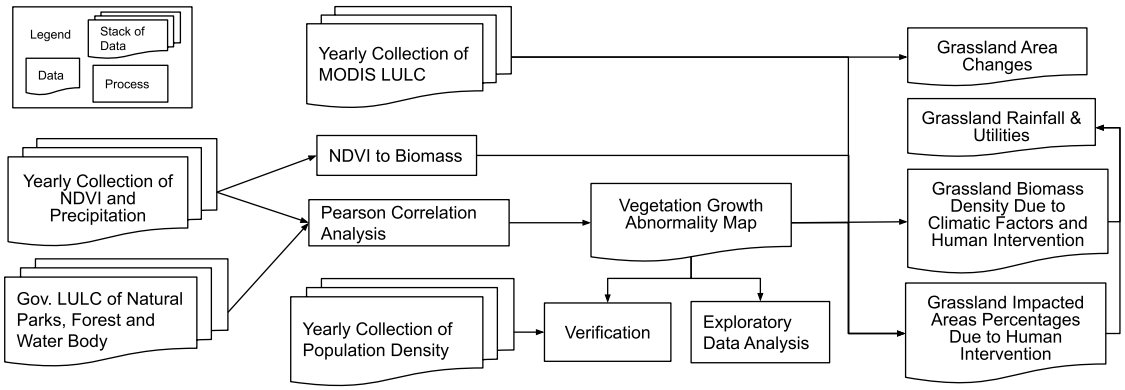

Figure 2.1 Flowchart for methodology

The first two subsections tell the logic and narrative behind the core model and the authors' arrangements in processing time-series data. With core ideas introduced, the third subsection gives a concise summary of data used in this research and workflow implemented in chronological order. All data used in this study are publicly accessible.

2.1 How Correlation between NDVI and Precipitation can be an indicator of Abnormality in Vegetation Growth

2.1.1 The intuition

In an ideal arid environment where the water source for vegetation is precipitation, the level of vegetation growth (NDVI) achievable is fundamentally decided by the amount of rainfall in the growing season (Bao et al., 2014; Dale et al., 2000; Ding et al., 2007; Jargalsaikhan, 2013; Sekiyama et al., 2015; Wang et al., 2003). But if we introduce a third-party influence like grazing or harvesting, vegetation growth would display a reduced or even reversed response from precipitation. Mongolia mainly consists of grassland and desert under arid and semi-arid climates, with pastoralism as the primary agricultural practice. Should we collect years of rainfall and vegetation growth records and calculate their trends, places that show a decrease in vegetation growth where precipitation is increasing can be deemed regions impacted by "third-party influences." That is, vegetation partially consumed by livestock. This easy-to-understand but naïve intuition has two fatal flaws that we must address. First, calculating trends requires a latent

assumption of monotonic change in the data. The NDVI and rainfall data are seasonal, and the year-by-year difference can fluctuate. The author conducted the Mann-Kendall test (Mann 1945; Kendall 1970) on the yearly data of NDVI and precipitation, only received a 25th percentile P Value of 0.097994 in rainfall and a median P Value of 0.144292 in NDVI, revoking the meaning of the trend calculation. Second, as stated in the previous paragraph, NDVI's reduced response from precipitation change is also a sign of third-party influence, which the intuition could not reflect. If we add additional rules as exceptions, the classification process to tell which parcel of land has vegetation growth loss would soon be too complex to be useful.

The writers' solution to this problem is correlation analysis. Given the direct causal relationship between NDVI and rainfall, any place free from third-party influences would show a good correlation value between these two data. When any disruption interrupts vegetation growth, resulting in reduced or even reversed response from precipitation, they all appeared as low or negative values in the correlation analysis. Thus, a complicated guessing problem is now a binary decision to tell if a place is left alone in its natural condition or heavily impacted by third-party influences, in our case, anthropogenic activities. We later called this correlation analysis as vegetation growth abnormality or, simply, abnormality.

2.1.2 Model verification

The verification of our results and model is in three progressive steps:
Step 1, with natural parks as a control group (free from agricultural and industrial production), we are to verify that high and low correlation values relate to good NDVI response to precipitation and reduced/reversed response in the latter case.

Step 2, using visual interpretation to find necessary but insufficient evidence of so-called "third-party influences" that caused a low correlation value. Our model is built on the assumption that industrial or agricultural human production disrupts vegetation's natural growth, so photographs of those sites can be helpful to solidify this paper.

Step 3, the geospatial dataset to cross-validate on the national scale. By the argument in the second step, if we find proof that higher population density links to a lower correlation value between NDVI and precipitation, we can prove our model stands firmly.

Because the hypothesis states that NDVI responds well to precipitation, water bodies and forest regions were excluded from the discussion in this paper because the former does not contain meaningful vegetation

information. The latter would have the issue of NDVI saturation (Liu et al., 2017), and livestock like horses and cows do not usually climb tall trees to eat the leaves.

2.2 Dealing with time-series data

2.2.1 Processing NDVI and precipitation data

Before conducting correlation analysis, we need to process the two participating data first. To represent vegetation growth each year, we select the maximum monthly composite as the value indicating the top growth the grass can reach within the timeframe for the given place. The reasoning behind this decision is that we must mask the seasonal fluctuation and focus on year-by-year change. Most vegetation growth and precipitation happen in synchronization during the summer seasons with a 3 to 4 weeks delay to precipitation events (Wang et al., 2003). The rainfall accumulated in the spring-summer period matters most to the vegetation growth during that year (Jargalsaikhan, 2013). And because NDVI in Mongolia usually peaks in August, subtracting the response delay, we use the maximum NDVI in the year and the sum-up value of GSMaP from April to July to conduct the correlation analysis, as suggested by other researchers mentioned in the Introduction (Ding et al., 2007).

To help understand the collection of 20-year data, we also computed the mathematical mean of NDVI and rainfall to explore the pattern behind those two data further. We conducted a geospatial correlation analysis between NDVI and Precipitation Mean. If our hypothesis holds, those two values display a high correlation because a higher amount of rainfall would always lead to higher vegetation growth. Another geospatial correlation we did is between NDVI Mean and the Correlation value for Growth Abnormality. Should there be any meaningful positive or negative correlation value, we can conclude that anthropogenic activities impact unevenly to sparsely or densely vegetated regions.

2.2.2 Processing population density and LULC data

And for processing population density data (LandScan), the 20 years of annual records were compressed into a single layer of mean value to represent the traces of human activities in Mongolia. Because our research focuses on the general vegetation growth of the grassland, we added two additional data preprocessing and analyzing procedures:

First, we did a 99^{th} percentile filtration of LandScan results. There is 30% population in Mongolia conducting herding activities covering around 60% of the land in Mongolia, yielding an average population density of about one person per square kilometer. Adding the consideration of small herders' towns, the authors consider the 99th percentile value of 3.8 people per square kilometer

very fitting.

Second, one of Mongolia's core ecological and environmental concerns is its grassland's sustainability. Using MODIS LULC data, we exclusively investigated the 20-year change in grassland expansion, average biomass, and precipitation change with the additional information from our Abnormality analysis results. 2001, 2005, 2010, 2015, and 2020 were selected and sampled for discussion.

Due to the data-acquiring pipeline, all data were organized in Geographic Coordinate System. Thus, any calculations based on areas were not available. Only ratio and average densities were presented.

2.3 Data Table and Technicality Workflow

Table 2.1 Data used in this study.

Data	Source	Temporal Coverage	Original Resolution
Population Density (LandScan Global)	ORNL	2001 ~ 2020	30 Arc Second (~1KM.), Yearly
NDVI (MODIS MOD13A3 2001~2019 MOD13A2 2020)	NASA – LP DAAC	2001 ~ 2020	1 KM., Monthly
LULC (MODIS MCD12Q1)	NASA – LP DAAC	2001 ~ 2020	500 M., Yearly
Precipitation (GSMaP)	JAXA	2001 ~ 2020	0.1 Degree Longitude/Latitude, Monthly
Waterbody, national parks, and forest	MN EIC	-	Vector file (.SHP)

M.: Meters, KM.: Kilometers, MODIS: The Terra and Aqua combined Moderate Resolution Imaging Spectroradiometer, LULC: Land Use Land Cover, NDVI: Normalized Difference Vegetation Index, NASA – LP DAAC: NASA Land Processes Distributed Active Archive Center, GSMaP: Global Satellite Mapping of Precipitation, JAXA: Japan Aerospace Exploration Agency, MN

Gov.: Mongolian Government, MN EIC: The Mongolian Environmental Information Center, ORNL: Oak Ridge National Laboratory.

Precipitation (GSMaP) Global Satellite Mapping of Precipitation (GSMaP) is a rainfall observation record based on several satellites by the Japan Space Agency (JAXA). We are using the GSMaP-Near Real-Time (NRT) v6 dataset originally at a monthly interval from 2001 to 2020 at a resolution of 0.1 Degree Longitude/Latitude (Kubota et al. 2020).

NDVI. The MODIS vegetation indices is a global data depicting vegetation canopy greenness generalizing information on leaf area, canopy structure, and chlorophyll. We chose this product for its comprehensive coverage, both temporarily and spatially. Study shows MODIS NDVI performs well with seasonal phenology (Huete et al., 2002). The specific data we used here is the Vegetation Indices Monthly L3 Global at a resolution of 1 KM. (MOD13A3 and MOD13A2) from 2001 to 2020 (Didan 2015).

LandScan Global. The LandScan program is an effort made by the US Oak Ridge National Laboratory to provide global population distribution data that reflect each country's unique case and satellite data to disaggregate the census data into population density within associated borders annually (Rose et al., 2021). Each pixel's digital value represents the estimated number of people in that area under the consideration of a 24-hour day cycle at a geospatial resolution of 1 Sqr. KM. We collected the data from 2001 to 2020.

LULC. The Terra and Aqua combined Moderate Resolution Imaging Spectroradiometer (MODIS) Land Cover Type (MCD12Q1) Version 6 data product (Friedl and Sulla-Menashe 2019) provides information on land cover types on a global scale from 2001 to 2020 at a resolution of 500 meters and yearly temporal intervals. The data we use implemented the International Geosphere-Biosphere Programme (IGBP) legend and class descriptions.

Borders, natural parks, lakes, and forests. Due to the need to find control group samples and inherent problems with NDVI and our theoretical model discussed later in this section, we also collected administration border and land type data provided by The Mongolia Environmental Information Center("EIC GeoNetwork") in the format of vector data layer (.shp files).

All data are acquired under Geographic Coordinate System in WGS 1984 format.

2.3.1 Preprocessing

Clipping and Data Value Rectification.

All collected data underwent clipping against the Mongolian border, and data values were checked against QA layers and documents.

For LandScan data, we are taking the average population density over the 20 years in the nomadic rural areas, so we did a 99th percentile filter to exclude large cities and towns.

For Precipitation data, we applied bilinear resampling to match with NDVI data.

For LULC data, we reclassified the data to simplify the class selection (Zhang et al., 2020) and selected IGBP type 6~11 as grassland. We later vectorized the selected pixels into points to extract values from other raster datasets.

For NDVI data, it is checked with the following formula:

$$NDVI_{rectified} = \begin{cases} NDVI * 0.0001 \\ Null\ if\ NDVI < -2000\ or\ NDVI > 10000 \end{cases} \quad (1)$$

Stacking data from monthly to yearly. NDVI and precipitation data's original temporal resolution is monthly, and we transformed them into yearly data for further calculation. The NDVI annual data was generated from the maximum value of a given year. According to existing research, yearly precipitation data was stacked by the total value from the growing season between April to July (Jargalsaikhan, 2013). The stacking operation is the usual mathematical summation following the formula:

$$Value_{stacked} = \sum_{t=1}^{T} Value_t \quad (2)$$

where t is the time unit of the target time.

Filtering of forests and lakes. The filtering mask was generated by subtracting vector data of forests and lakes from the Mongolia border vector file. NDVI, Precipitation, LULC, and Population Density datasets were filtered against this mask.

2.3.2 Temporal Pearson Correlation – the Abnormality Index and accompanying calculation

Correlation calculation. We use the maximum NDVI in the year and the sum-up value of Precipitation (GSMaP) from April to July to calculate the Temporal Pearson Correlation between those two factors over all of Mongolia between 2001 and 2020.

The cutout for coefficients of meaningful correlation is at +0.3 and -0.3 (Ratner, 2009).

The calculations of Pearson Correlation follow the definition form:

$$\rho_{X,Y} = \frac{\sum XY - \frac{\sum X \sum Y}{N}}{\sqrt{\left(\sum X^2 - \frac{(\sum X)^2}{N}\right)\left(\sum Y^2 - \frac{(\sum Y)^2}{N}\right)}} \quad (3)$$

Exploratory data analysis. The mean, maximum, minimum, standard deviation, fifth percentile, first quantile, third quantile, 95th percentile, and skewness were calculated. Then we conducted geospatial correlation analysis by taking

pairs of pixels at the exact location across two layers as the input for calculation. We did the two pairs of geospatial correlations to explore the characteristics of the data and results, the postfix "-Mean" is the yearly mean:

- NDVI-Mean vs. Correlation: We want to know if bare lands and bushy areas show the same level of abnormality.
- NDVI-Mean vs. Precipitation-Mean: Reconfirm that precipitation is the limiting factor of vegetation growth in Mongolia. Should this assumption hold, there would be a significant positive correlation between those two layers.

Grassland evaluation with the correlation results. The average biomass, precipitation, percentages of the abnormal growth area, and growth rate of the grassland were calculated in the years 2001, 2005, 2010, 2015, and 2020. Using the vectorized point data from LULC data, we can extract related NDVI, rainfall, and correlation value to tables and then put them into data processing software to get the results.

Following a previous study (Sekiyama et al., 2015), the NDVI to Biomass transformation is in this formula:

$$Biomass = 247.3 \times NDVI + 14.7 \quad (4)$$

Biomass is in Tons per Sqr. KM. The average precipitation it takes to grow a unit density of biomass, referred to as the rainfall utility number, was also calculated and appended in the result table.

2.3.3 Verification

Verification with Temporal Point Sampling. First, we are conducting so-called temporal point sampling by picking up two sets of three points of records in the monthly data collection across all 20 years.

- Site in Natural Parks with Positive Correlation between Precipitation and NDVI: This is our controlling group because natural parks can be viewed as places protected from human disturbances like mining or grazing.
- Site Outside Parks with No Correlation between Precipitation and NDVI: This is our observing window for places potentially disrupted by human activities.

Three points of each set would be averaged as the representation of each group, with related time-series charts drawn. Due to visualization limitations, the year 2020 monthly records were emitted.

Verification with Visual Interpretation. Then, using Google Earth, we selected three investigation areas covering the East, Central, and South regions to find visual evidence of potential disruptions from human settlement footprints.

Verification with LandScan Data. After filtration of the 99th percentile value in LandScan data, the layers of LandScan and Correlation were put into scatter plot and regression analysis.

All the work is done with the software and tools listed below:

ArcGIS(Version 10.7.1), System for Automated Geoscientific Analyses (SAGA), Jupyter (Kluyver et al., 2016), PANDAS (McKinney 2010), and Matplotlib (Hunter 2007).

3. Results

3.1 Growth Abnormality: NDVI-Precipitation Correlations and Exploratory Data Analysis

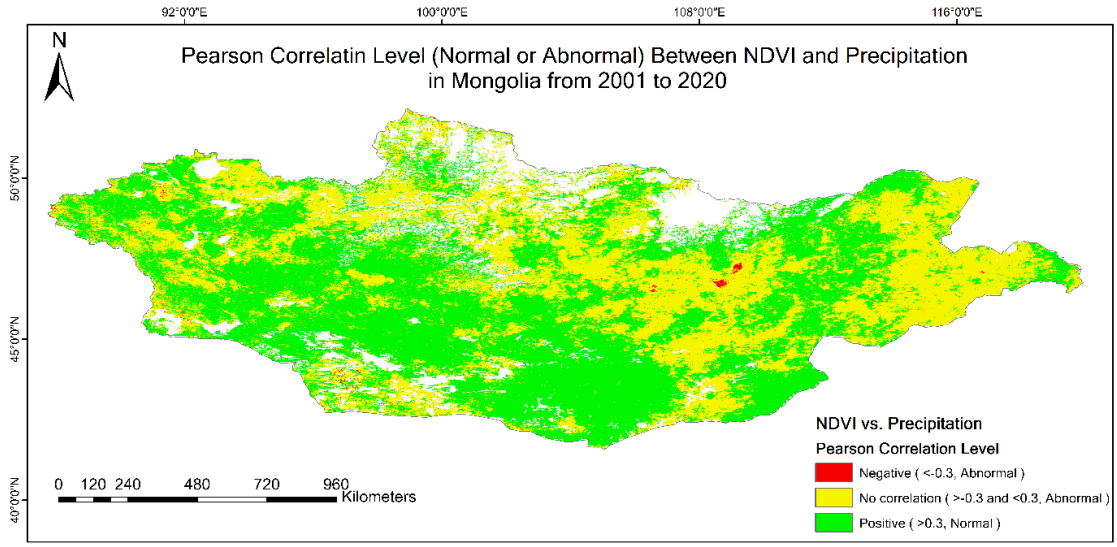

Figure 3.1 The Temporal Pearson Coefficients between NDVI and Precipitation from 2001 to 2020, the cutout is 0.3 and -0.3. The positive correlation is considered normal in vegetation growth, whereas other groups are deemed abnormal.

From our cutouts of the correlation described previously, places with higher than 0.3 values are deemed normal growth areas. All the pixels counted as "positive relationships" can be observed across the correlation map in figure 3.1. Other pixels not displaying meaningful correlations even have negative correlations that appear to form a belt area from upper West to Central. The bulging eastern corner is also harboring large regions in abnormal conditions. This map is produced based on the continuous correlation value map (Figure A2) to alleviate readers' burden. Please refer to the Appendix if you are interested to know the whole range of temporal NDVI-Precipitation correlation values in Mongolia.

Table 3.1 Quantiles and Descriptive Statistics of NDVI-Precipitation Correlation

Minimum	-0.811	**95-th percentile**	0.654
5-th percentile	-0.015	**Maximum**	0.931
Q1	0.190	**Standard deviation**	0.204
Median	0.331	**Mean**	0.327
Q3	0.475	**Skewness**	-0.223

The descriptive statistics in table 3.1 show a -0.223 negative skewness to the left, which means most pixels are prone to be positive. The fifth percentile is -0.015, which means we can infer that only a tiny area of Mongolia displayed a negative relationship between NDVI and precipitation. Moreover, the 3rd Quartile is 0.475, and the 95th percentile is 0.654 with a median value of 0.331, so there is a large amount (roughly half of all pixels) of places displaying a somewhat good correlation between Rainfall and NDVI.

Table 3.2 Geospatial Correlation Between NDVI Mean, Growth Abnormality, and Precipitation Mean

Data Pair	NDVI-Mean vs. Precipitation-Mean	NDVI-Mean vs. Abnormality
Correlation Value	0.896	-0.223

The significantly high positive correlation between NDVI Mean and Precipitation Mean data in table 3.2 indicates that vegetation flourishes in places of high rainfalls in the growing season of Spring to Summer, which confirms this research's assumption that rainfall is a critically limiting factor of vegetation growth in Mongolia. The weakly significant negative value between NDVI-Mean and the Abnormality Map indicates that places with higher vegetated areas manifest more disturbances and abnormalities in flora growth.

3.2 Grassland Changes 2001 to 2020

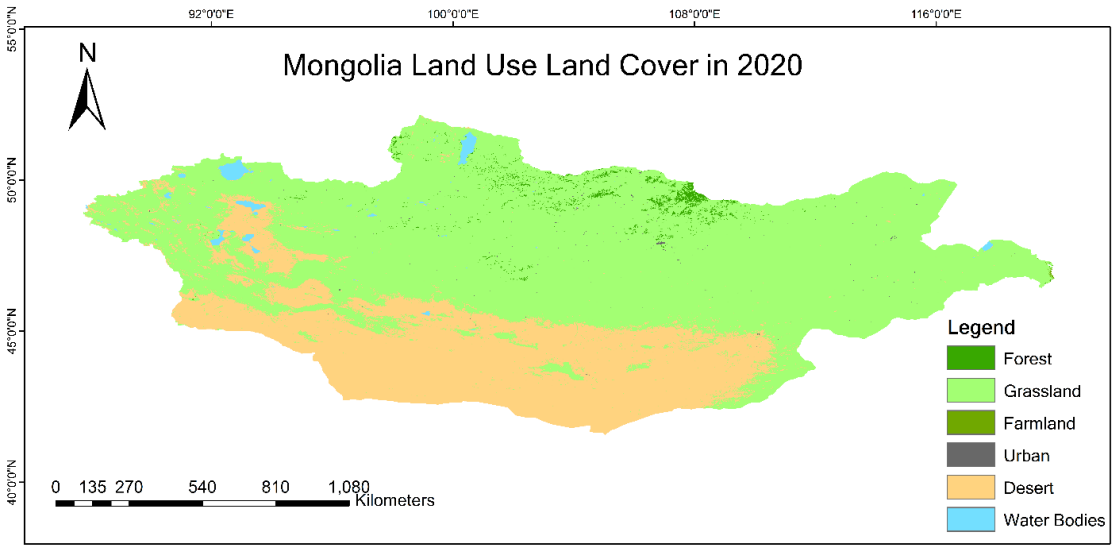

Figure 3.2 LULC of Mongolia in 2020

Table 3.3 Mongolia Grassland Related Yearly Change Data

Year	2001	2005	2010	2015	2020
Grassland Area Growth[1]	-	0.37%	1.81%	3.05%	4.69%
The ratio of Abnormal Region	51.48%	51.30%	51.29%	50.91%	50.89%
Average Biomass in Abnormal Region (Metric Ton per Sqr. KM)	120	124	126	128	141
Average Biomass in Normal Region (Metric Ton per Sqr. KM)	111	116	116	119	129
Average Precipitation in Abnormal Region (unit: mm)	215	222	161	274	295
Average Precipitation in Normal Region (unit: mm)	183	200	147	227	269
Precipitation/Per Biomass Density in Abnormal Region (Unit mm/Ton per Sqr. KM)	1.778	1.784	1.268	2.131	2.086
Precipitation/Per Biomass Density in Normal Region (Unit mm/Ton per Sqr. KM)	1.636	1.714	1.257	1.897	2.072

[1]Year 2001 as the base.

Figure 3.2 Land Use Land Cover (LULC) map of Mongolia in 2020 gives us the current distribution of land classes and the general combination of terrain and climates. This is for general reference. As for records of 2001, 2005, 2010, and 2015 LULC, please reference figure A1 in the appendix. From figure 3.2, we can see that the desert resides in the dry Gobi South and West. The rest of

the country is grassland, with a handful of forests in the Central Northern region. Over the twenty years from 2001, the area of grassland has extended by around 4.69%, according to the MODIS LULC data in table 3.3. The ratio of the area deemed as abnormal vegetation growth is about the same over the 20 years. From the average biomass data, we can see overall that the grassland is getting greener over the years, which is explained by the rising average precipitation. However, rainfall and biomass are lower in the NORMAL region, similar to the geospatial correlation results between NDVI Mean and Abnormality we discovered in section 3.1. The Precipitation/Per Biomass Density is our calculation of, on average, how much precipitation it takes to grow a unit density of biomass in grassland. We later reference this result as the rainfall utility number.

3.3 Verification

Our three-step progressive verification process is explained in the method section. First, in the resulting group (a), we find that a good correlation level from our calculation stands for NDVI's good seasonal and yearly response to changes in precipitation, especially compared with the no correlation non-park site that is considered disturbed by non-climatic factors. Unlike the saw-like shape of the control group figure 3.3 (a)-(2) NDVI line, the No Correlation site shows a weird "flat-roof" NDVI line despite the changes in precipitation.

Then, in results group (b), we find visual cues of human presence in places marked as No Correlation or Negative Correlation between NDVI and Precipitation from Google Earth.
The Coordinates of those five sites are:

1. 43°35'17.86" N 103°51'48.77" E
2. 48°17'41.09" N 93°36'42.06" E
3. 47°03'08.00" N 116°19'16.79" E
4. 47°11'12.65" N 109°11'47.38" E
5. 42°45'27.88" N 98°48'50.74" E

And for result in (c), with increasing population density, the Correlation Values are converging towards the No Correlation cutouts with the linear regression of

$$Correlation = 0.330 - 0.008 \times LandScan$$

With R^2 = 0.07%, we can conclude that our model's result:

- Captures the abnormal response of NDVI to precipitation changes.
- Where human presence can be spotted.
- And the abnormality is linked to increases in human population density.

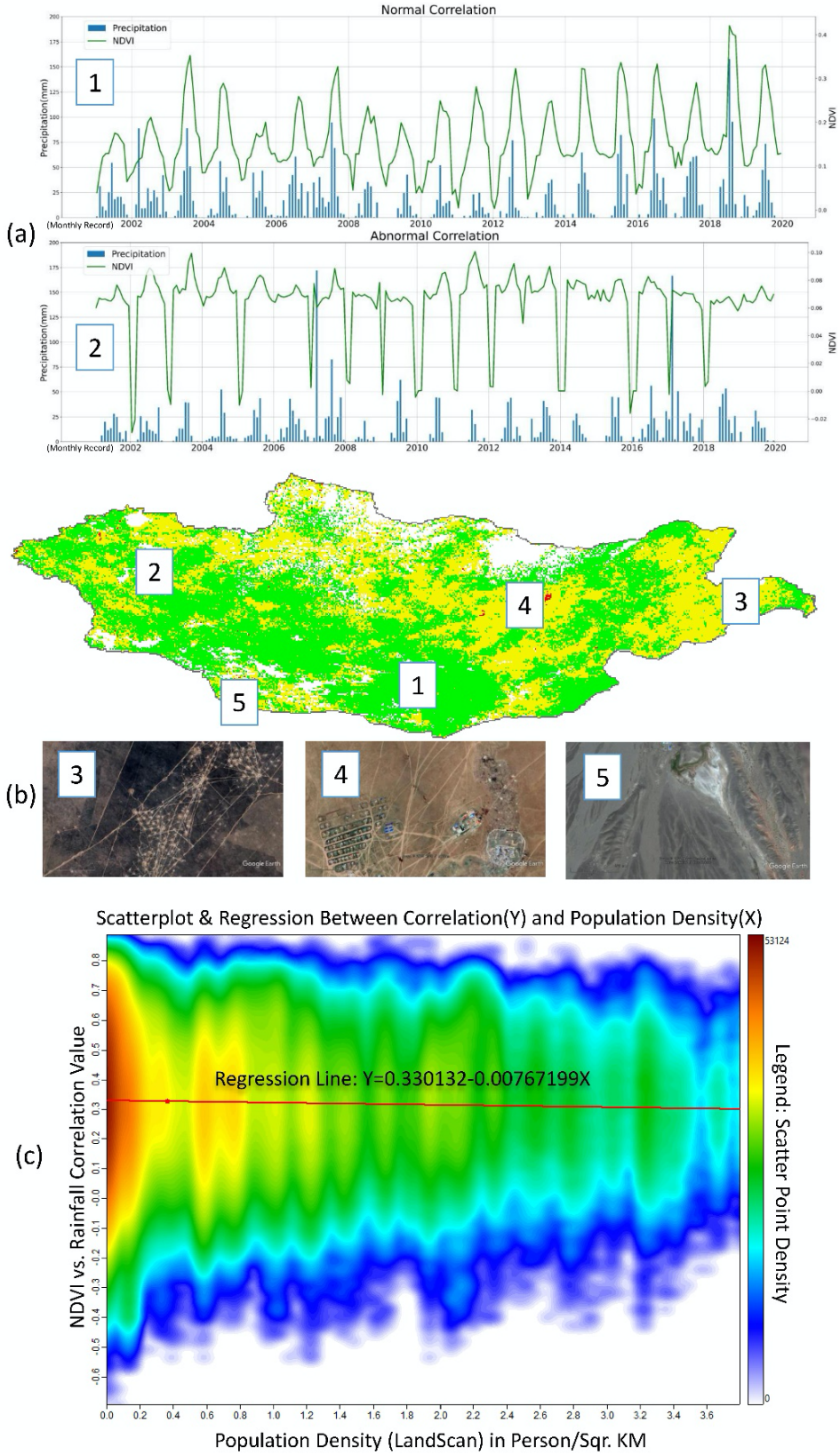

Figure 3.3 Results from the verification process. The map in the middle marked out the location of the sampling sites with related numbering on both the charts/images and the map of Abnormality in the middle. (a) The monthly precipitation and NDVI records of

sample sites in Natural Parks with Positive Correlation level (1) and Non-park No Correlation sample site (2), Precipitation is drawn in the bar chart, and the green line is the NDVI in the monthly charts, the figures are capped at 200 mm for Precipitation; (b) Three photo of residential/production sites (3) (4) (5) on the abnormal region in the map; (c) Scatterplot with density coloring and Linear Regression between the Abnormality Correlation Value and Population Density, the liner regression is marked with a red line and printed in the graph.

4. Discussion

4.1 The Causal Relationship and the Abnormality Map Evaluation

It is a known fact that correlation does not equate to causality. However, in our case of precipitation and vegetation growth, it is a biological fact that precipitation is the defining factor in vegetation growth, as in all living creatures on this planet. The geospatial correlation between NDVI-Mean and Precipitation-Mean in table 3.2 is conclusive proof of this claim. With a high 0.896 value in correlation, this is quantitative evidence that vegetation growth follows rainfall's footsteps in Mongolia despite possible differences in altitude. This indicates that places with high precipitation values also see high vegetation coverage. With the causal relationship understood, simple correlation analysis can be used to distinguish between disrupted and undisrupted vegetated areas.

For the NDVI-Precipitation Temporal Pearson Correlations in figure 3.1, the pixels categorized as meaningful positive or negative groups are not that high in the Temporal Pearson Correlation scale. Half of the pixels display no correlation between vegetation growth and rainfall, indicating third-party interference during the research period. And we interpreted that observed vegetation growth responded better in the South, but it does not mean vegetation grows better in such cases. Our geospatial correlation analysis shows a negative correlation between NDVI-Mean and Abnormality in table 3.2. It means a place with a higher average NDVI value would be more likely to see a lower NDVI-Precipitation correlation value, indicating a tendency of disrupted vegetation growth. Then this number tells us that in Mongolia, places with higher vegetation coverage are more fitting for grazing and are the places receiving negative impacts on vegetation growth. Given the agricultural landscape of Mongolia, it is most likely human activities, especially the animal husbandry industry. This is excellent evidence that anthropogenic activities like grazing are putting heavy stress on the local environment.

Another vital point of the model result is that the distribution of abnormality is a historical evaluation, which means that places marked as anomalies might not be as damaged in the current year, so the analysis is a retrospective review under the 20 years timeframe. The meaningful/insignificant correlation line cutout values of 0.3 and -0.3 are of empirical convenience, so places deemed as normal or positive relationships are not free from disruptions like harvesting or grazing; they are simply different in degrees of disturbances. This critical insight is stressed in the background of exploding number of livestock from 2001 to 2020 and our analysis in the following subsection.

4.2 Grassland Changes

Over the years, from 2001 to 2020, there has been a slight expansion of grassland in Mongolia by around 5 percent in table 3.3. This increase is likely contributed by the retreat of desert in the South, as indicated by our 20 years of MODIS LULC data of Mongolia (See Appendix Table A1). With the growing size of the grassland, percentages of being abnormal have dropped slightly, which might come from those newly reclaimed land from the desert by the advancing grassland.

The data table 3.3 shows that the average biomass density increases with precipitation. So we can assume the increased rainfall is why the grassland areas and biomass density are growing. However, biomass density and precipitation are higher in the category of abnormal growth region than the usual places. This can be interpreted as the more vegetated areas would be in the priorities to graze upon. Though the precipitation is increasing in our records, this seems still surprising to see the average biomass density increasing, given an almost three-time increase in the total number of livestock in the past twenty years (“Livestock,” NSO of Mongolia). One explanation of our data is summarized in the data table of section 3.2 as the rainfall utility number.

The rainfall utility data tells the average precipitation it takes to grow a unit of biomass in the grassland. We can see that places in the abnormal region always carry more water to produce a unit of grassland biomass. This tells us that there should be more biomass in the natural environment if there are not so many disturbances or grazing activities. And we can see that with more precipitation and higher biomass density, it takes more rainwater to grow a unit of grassland biomass in both abnormal and normal regions. Given the exploded number of livestock mentioned in section 1.1 background, we can view this as evidence that grazing activities are intensifying.

The author is happy to see the actual

increase in vegetation coverage in Mongolia despite the ever-higher burdens of added livestock. We argue that the rise of precipitation would be a good chance to lower grazing intensity to let the grassland recover in Mongolia for future sustainable development.

4.3 Verification Evaluation

Though other researchers and institutions' research and statistical data show that our abnormality map has a resemblance to cattle distribution, land type, and land degradation (Meng et al., 2020; Liu et al., 2013; "Desertification and Land degradation in Mongolia," NEASPEC), we hope to have our quantitative discussion.

Mongolia's vastness and the COVID pandemic's impact put a high bar against large-scale ground investigations. And one of the research referenced by this paper lacks a control group (Sekiyama et al., 2015). To overcome the shortcomings, we took two assumptions: population density in the rural area would link to nomadic production; two, places within the natural park are well-protected from human disturbances by the law and can be used as a substitute for control groups. So, the first step of verifying our model is to check the monthly records to be sure the correlation levels are a good indicator of the abnormal relationship between NDVI and precipitation.

With Temporal Point Sampling in figure 3.3 group (a), we can see that:
The no correlation group showed a characteristic " flat-roof " phenomenon meaning the vegetation growth did not respond well to the changes in precipitation during the year, forming a flatline over changing precipitation numbers. We think the reason can be either the rainfall is too small to make an impact, the vegetation was grazed constantly to a low biomass number or the result of irrigation. The NDVI's responses to precipitation are much more apparent in the Park Positive group to a more iconic seasonal curve. Differences in year-by-year precipitation events also lead to higher NDVI values in this group. This confirms that our model's results are a good indicator for regular and irregular NDVI-Precipitation relationships.

For step two, in the (b) group of figure 3.3, we successfully located visually human presence via Google Earth. We are linking the abnormal relationship between NDVI and rainfall to human existence. But this is necessary but not sufficient evidence, and we need national-level confirmation.

The Population Density (LandScan) – Abnormality scatters plot shows that with population density increase, the respective NDVI-Precipitation correlation value would converge negatively below 0.3 in

figure 3.3 group (c). And the regressed line also indicates this trend. The author's interpretation is that increased population density leads to more nomadic activities, which disturbs the area's vegetation growth and leads to a lower correlation value between precipitation and NDVI. This negative regression line verified the effectiveness of our model and results. We do notice low R-squared values. The reason for that could be the caveats in LandScan itself. The data is disaggregated from census data into density distribution by remote sensing data and other GIS information like road networks. The data does not directly represent the population residing in the wilderness of Mongolia.

4.4 Methods Discussion, Limitations, and Next Steps

Compared with previous research on vegetation growth response to climatic factors in Mongolia (Sekiyama et al., 2015; Jargalsaikhan, 2013), this research extends the geospatial and temporal scales. By selecting the time window of the first two decades, we made our results more closely related to the current situation. The observation is beyond the North-South single direction by covering the whole country, leading to insights covering the changes in East-West and North-South directions.

Our research also jumped out of the traditional comparison research that only tells the increase or decrease of vegetation growth, ignoring the underlying impact of anthropogenic activities. Like in section 4.3, we successfully uncovered that beneath the increased greenness due to a higher level of precipitation, the utility value of rain in biomass and our Vegetation Growth Abnormality map revealed the burdens and wasted recovering potential by an ever-increasing number of livestock from 2001 to 2020.

Yet there are several limitations the authors like to address. First, we would like to talk about our study's confidence level. All the data involved in the calculation, discussion, and verification have their range of quality assurance. Our interpretation of the correlation results is limited by the data collected. The [-0.3, 0.3] cutout in correlation values is an empirical attempt to draw the threshold of "meaningful correlation." There is still much to debate about the fitting cutouts because we are using 20 pairs of two decades of annual data. The temporal correlation analysis could potentially be more representative if we are using seasonal or bi-monthly data points. This would require careful investigation in our next research steps. Should we have ground truth concerning accurate human footprint, e.g., nomadic tent house distribution, caveats from data like LandScan can be circumvented, increasing our confidence in the results. Producing such a dataset is the authors' goal for future efforts.

Moreover, temporal point sampling is the authors' attempt to gain insight into the 20-year-long time-series data; the observation is severely limited by the selected samples' number and distribution. It is challenging to balance the cost of sampling and the representative strength of the samples. The authors are confident that we can further strengthen the discussion by a more substantial number of more evenly distributed samples selection with added ground truth data like yearly nomadic tent house distribution collection in future research.

5. Conclusion

To investigate the sustainability and stability of the natural environment, especially grassland in Mongolia, the authors propose a method of using NDVI's response to precipitation across yearly data collection to measure the abnormality of vegetation growth potentially caused by human disturbances (most likely, grazing). We calculated the Vegetation Growth Abnormality map from the Temporal Pearson Correlation Value between NDVI and Precipitation data in Mongolia from 2001 to 2020. Then we factored in MODIS LULC data to calculate the grassland's growth rate, the ratio of abnormal vegetation growth, average historical precipitation, and biomass density in Mongolia during the same period. Finally, we finished the verification discussion with sampling in monthly records, aerial photo inspection, and population density data.

We found that the mean and median values of NDVI-Precipitation in Mongolia from 2001 to 2020 are 0.327 and 0.331, with a standard deviation of 0.204. Grassland has grown 4.69% in the twenty years with increased biomass density and average precipitation. About 51% of grassland is deemed abnormal in vegetation growth, possessing a higher biomass density and moderate rainfall than the other normal half. Besides visual confirmation of human presence in regions classified as Abnormal Vegetation Growth regions, we have a negative linear regression between population density and NDVI-Precipitation Correlation Value of Correlation = 0.330-0.008 × LandScan, linking low correlation value to higher population density and intensified anthropogenic activities behind such numbers.

The authors conclude that negative third-party influences like grazing are widespread because around half of the pixels in the correlation map and grassland show abnormal relationships between precipitation and NDVI. The precipitation/biomass ratios in both normal and abnormal growth regions in grassland are growing, hinting that a higher portion of growth potential is consumed; the explosion of livestock

numbers in Mongolia did put heavy stress on the local environment in the first two decades of the 21st century even though NDVI data suggest Mongolia is getting greener.

The authors are looking forward to incorporating additional datasets and methods to directly count grazing costs to the local environment geospatially in our future research. One of the directions is nomadic tent house detection and location research.

Acknowledgments

This study was supported by JST SPRING, Grant Number JPMJSP2108.

References

[1] Angerer, Jay, Guodong Han, Ikuko Fujisaki, and Kris Havstad. "Climate change and ecosystems of Asia with emphasis on Inner Mongolia and Mongolia." Rangelands 30, no. 3 (2008): 46-51. https://doi.org/10.2111/1551-501X(2008)30[46:CCAEOA]2.0.CO;2

[2] Bao, Gang, Zhihao Qin, Yuhai Bao, Yi Zhou, Wenjuan Li, and Amarjargal Sanjjav. "NDVI-based long-term vegetation dynamics and its response to climatic change in the Mongolian Plateau." Remote Sensing 6, no. 9 (2014): 8337-8358. https://doi.org/10.3390/rs6098337

[3] Beck, Hylke E., Niklaus E. Zimmermann, Tim R. McVicar, Noemi Vergopolan, Alexis Berg, and Eric F. Wood. "Present and future Köppen-Geiger climate classification maps at 1-km resolution." Scientific data 5, no. 1 (2018): 1-12. https://doi.org/10.1038/sdata.2018.214

[4] Carlson, Toby N., and David A. Ripley. "On the relation between NDVI, fractional vegetation cover, and leaf area index." Remote sensing of Environment 62, no. 3 (1997): 241-252. https://doi.org/10.1016/s0034-4257(97)00104-1

[5] Dale, Virginia H., Linda A. Joyce, Steve McNulty, and Ronald P. Neilson. "The interplay between climate change, forests, and disturbances." Science of the total environment 262, no. 3 (2000): 201-204. https://doi.org/10.1016/s0048-9697(00)00522-2

[6] Densambuu, B., S. Sainnemekh, B. Bestelmeyer, and U. Budbaatar. "National report on the rangeland health of Mongolia: Second Assessment." Green Gold-Animal health project, SDC (2018): 62.

[7] North-East Asian Subregional Programme for Environmental Cooperation (NEASPEC). “Desertification and Land degradation in Mongolia.” Retrieved May 10, 2022, from https://neaspec.org/sites/default/files/1.2 Ms. Mandakh Nyamtseren.pdf

[8] Ding, Mingjun, Yili Zhang, Linshan Liu, Wei Zhang, Zhaofeng Wang, and Wanqi Bai. "The relationship between NDVI and precipitation on the Tibetan Plateau." Journal of Geographical Sciences 17, no. 3 (2007): 259-268. https://doi.org/10.1007/s11442-007-0259-7

[9] Didan, Kamel. "MOD13A3 MODIS/Terra Vegetation Indices Monthly L3 Global 1km SIN Grid V006" [Data set]. NASA EOSDIS Land Processes DAAC (2015). https://doi.org/10.5067/MODIS/MOD13A3.006

[10] Didan, Kamel. "MOD13A2 MODIS/Terra Vegetation Indices 16-Day L3 Global 1km SIN Grid V006" [Data set]. NASA EOSDIS Land Processes DAAC (2015). https://doi.org/10.5067/MODIS/MOD13A2.006

[11] Friedl, Mark, & Sulla-Menashe, Damien. "MCD12Q1 MODIS/Terra+Aqua Land Cover Type Yearly L3 Global 500m SIN Grid V006" [Data set]. NASA EOSDIS Land Processes DAAC (2019). https://doi.org/10.5067/MODIS/MCD12Q1.006

[12] EIC GeoNetwork. (n.d.). [Data set] Retrieved February 26, 2021, from http://portal.eic.mn:8080/geonetwork/srv/eng/catalog.search#/home

[13] Rose, A., McKee, J., Sims, K., Bright, E., Reith, A., & Urban, M. "LandScan Global 2020 [Data set]." Oak Ridge National Laboratory (2021). https://doi.org/10.48690/1523378

[14] Huete, Alfredo, Kamel Didan, Tomoaki Miura, E. Patricia Rodriguez, Xiang Gao, and Laerte G. Ferreira. "Overview of the radiometric and biophysical performance of the MODIS vegetation indices." Remote sensing of environment 83, no. 1-2 (2002): 195-213. https://doi.org/10.1016/s0034-4257(02)00096-2

[15] Hunter, John D. "Matplotlib: A 2D graphics environment." Computing in science & engineering 9, no. 03 (2007): 90-95. https://doi.org/10.1109/mcse.2007.55

[16] Jargalsaikhan, Luvsandorjiin. "Long-term study of the relationship between precipitation and productivity in the main pasture vegetation of a steppe ecosystem in Eastern Mongolia." The Mongolian ecosystem network (2013): 33-42. https://doi.org/10.1007/978-4-431-54052-6_4

[17] Kendall, M. G. "Rank correlation methods." (1948).

[18] Kluyver, Thomas, Benjamin Ragan-Kelley, Fernando Pérez, Brian E. Granger, Matthias Bussonnier, Jonathan Frederic, Kyle Kelley et al. Jupyter Notebooks-a

publishing format for reproducible computational workflows. Vol. 2016(2016): 87-90. https://doi.org/10.3233/978-1-61499-649-1-87

[19] Kubota, Takuji, Kazumasa Aonashi, Tomoo Ushio, Shoichi Shige, Yukari N. Takayabu, Misako Kachi, Yoriko Arai et al. "Global Satellite Mapping of Precipitation (GSMaP) products in the GPM era." Satellite precipitation measurement (2020): 355-373. https://doi.org/10.1007/978-3-030-24568-9_20

[20] Liu, Shiliang, Fangyan Cheng, Shikui Dong, Haidi Zhao, Xiaoyun Hou, and Xue Wu. "Spatiotemporal dynamics of grassland aboveground biomass on the Qinghai-Tibet Plateau based on validated MODIS NDVI." Scientific reports 7, no. 1 (2017): 1-10. https://doi.org/10.1038/s41598-017-04038-4

[21] Liu, Yi Y., Jason P. Evans, Matthew F. McCabe, Richard AM De Jeu, Albert IJM van Dijk, Albertus J. Dolman, and Izuru Saizen. "Changing climate and overgrazing are decimating Mongolian steppes." PloS one 8, no. 2 (2013): e57599. https://doi.org/10.1371/journal.pone.0057599

[22] Mongolian Statistical Information Service of National Statistics Office of Mongolia (NSO). “Livestock Annual Number.” Retrieved February 10, 2021, from https://1212.mn/Stat.aspx?LIST_ID=976_L10_1

[23] Maekawa, Ai. "The cash in cashmere: Herders’ incentives and strategies to increase the goat population in post-socialist Mongolia." The Mongolian Ecosystem Network (2013): 233-245. https://doi.org/10.1007/978-4-431-54052-6_17

[24] Mann, Henry B. "Nonparametric tests against trend." Econometrica: Journal of the econometric society (1945): 245-259. https://doi.org/10.2307/1907187

[25] McKinney, Wes. "Data structures for statistical computing in python." In Proceedings of the 9th Python in Science Conference, vol. 445, no. 1 (2010): 51-56. https://doi.org/10.25080/majora-92bf1922-00a

[26] Meng, Xiaoyu, Xin Gao, Shengyu Li, and Jiaqiang Lei. "Spatial and temporal characteristics of vegetation NDVI changes and the driving forces in Mongolia during 1982–2015." Remote Sensing 12, no. 4 (2020): 603. https://doi.org/10.3390/rs12040603

[27] Mirza, M. Monirul Qader. "Climate change and extreme weather events: can developing countries adapt?" Climate policy 3, no. 3 (2003): 233-248. https://doi.org/10.3763/cpol.2003.03

30

[28] Food and Agriculture Organization of the United Nations. “Mongolia at a glance.” Retrieved February 26, 2021, from https://www.fao.org/mongolia/fao-in-mongolia/mongolia-at-a-glance/en/

[29] Nanzad, Lkhagvadorj, Jiahua Zhang, Battsetseg Tuvdendorj, Mohsen Nabil, Sha Zhang, and Yun Bai. "NDVI anomaly for drought monitoring and its correlation with climate factors over Mongolia from 2000 to 2016." Journal of arid environments 164 (2019): 69-77. https://doi.org/10.1016/j.jaridenv.2019.01.019

[30] Natsagdorj, L., D. Jugder, and Y. S. Chung. "Analysis of dust storms observed in Mongolia during 1937–1999." Atmospheric Environment 37, no. 9-10 (2003): 1401-1411. https://doi.org/10.1016/s1352-2310(02)01023-3

[31] Nyamsuren, Baasankhuu, Kenlo Nishida Nasahara, Takuji Kubota, and Takeshi Masaki. "Vegetation Mapping by Using GPM/DPR over the Mongolian Land." Remote Sensing 11, no. 20 (2019): 2386. https://doi.org/10.3390/rs11202386

[32] Pettorelli, Nathalie, Jon Olav Vik, Atle Mysterud, Jean-Michel Gaillard, Compton J. Tucker, and Nils Chr Stenseth. "Using the satellite-derived NDVI to assess ecological responses to environmental change." Trends in ecology & evolution 20, no. 9 (2005): 503-510. https://doi.org/10.1016/j.tree.2005.05.011

[33] Mongolian Statistical Information Service of National Statistics Office of Mongolia (NSO). “POPULATION OF MONGOLIA.” Retrieved February 10, 2021, from http://www.1212.mn/tables.aspx?TBL_ID=DT_NSO_0300_027V1

[34] Ratner, Bruce. "The correlation coefficient: Its values range between+ 1/− 1, or do they?" Journal of targeting, measurement and analysis for marketing 17, no. 2 (2009): 139-142. https://doi.org/10.1057/jt.2009.5

[35] Sekiyama, A., S. Shimada, M. Yokohama, and H. Toyoda. "Biomass estimation using MODIS imagery and its response to precipitation in Mongolian grasslands." Tokyo University of Agriculture Journal of agriculture science, 60(2015): 28-33.

[36] Shao, Y., and C. H. Dong. "A review on East Asian dust storm climate, modelling and monitoring." Global and Planetary Change 52, no. 1-4 (2006): 1-22. https://doi.org/10.1016/j.gloplacha.2006.02.011

[37] Stott, Peter. "How climate change affects extreme weather events." Science 352, no. 6293 (2016): 1517-1518.

https://doi.org/10.1126/science.aaf7271

[38] Tulokhonov, A. K., B. Z. Tsydypov, A. L. Voloshin, D. Zh Batueva, and Ts Chimeddorj. "Spatio-temporal characteristics of vegetation cover of arid and semiarid climatic zones in mongolia on the basis of vegetation index NDVI." Arid Ecosystems 4, no. 2 (2014): 61-68. https://doi.org/10.1134/s2079096114020115

[39] Wang, Jida, Paul M. Rich, and Kevin P. Price. "Temporal responses of NDVI to precipitation and temperature in the central Great Plains, USA." International journal of remote sensing 24, no. 11 (2003): 2345-2364. https://doi.org/10.1080/0143116021015481 2

[40] Zhang, Baolin, Atsushi Tsunekawa, and Mitsuru Tsubo. "Contributions of sandy lands and stony deserts to long-distance dust emission in China and Mongolia during 2000–2006." Global and Planetary Change 60, no. 3-4 (2008): 487-504. https://doi.org/10.1016/j.gloplacha.2007.06.001

[41] Zhang, Yanzhen, Qian Wang, Zhaoqi Wang, Yue Yang, and Jianlong Li. "Impact of human activities and climate change on the grassland dynamics under different regime policies in the Mongolian Plateau." Science of the Total Environment 698 (2020): 134304. https://doi.org/10.1016/j.scitotenv.2019.134304

[42] Zhao, X., K. Tan, S. Zhao, and J. Fang. "Changing climate affects vegetation growth in the arid region of the northwestern China." Journal of Arid Environments 75, no. 10 (2011): 946-952. https://doi.org/10.1016/j.jaridenv.2011.05.007

Appendix

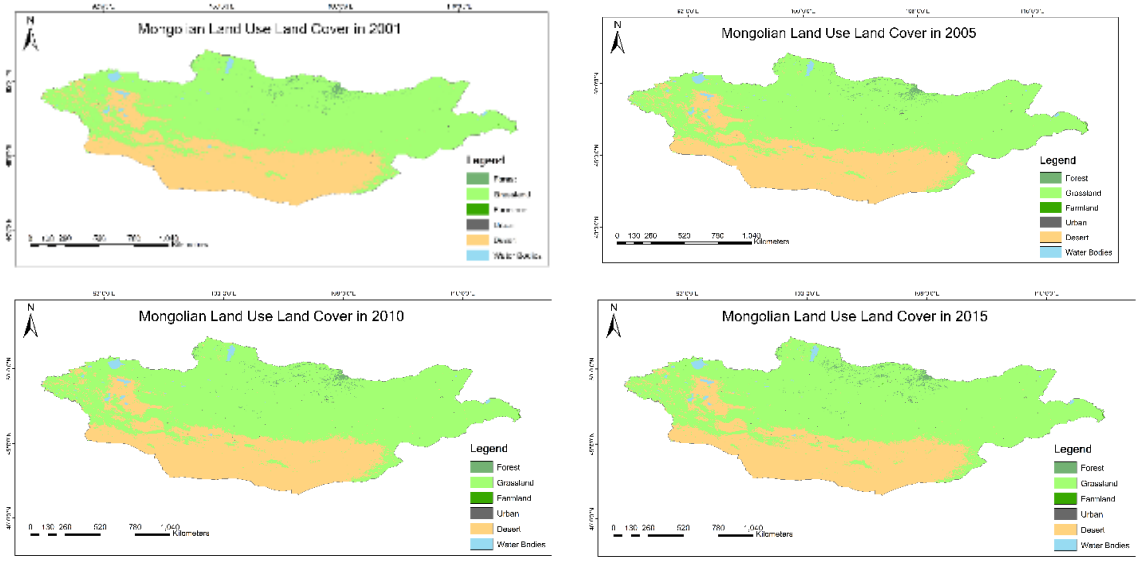

Figure A1. MODIS LULC map of Mongolia in 2001(upper left), 2005(upper right), 2010(lower left), and 2015(lower right).

Table A1. Pixel count for MODIS LULC of Mongolia 2001-2020.

Year	Forest	Grassland	Farmland	Urban built-up	Desert	Waterbody
2001	73810	7090715	1930	6886	3385678	87047
2002	73326	7113631	2000	6886	3363438	86785
2003	71450	7136473	1918	6886	3342688	86651
2004	71223	7130339	1965	6888	3349499	86152
2005	69848	7117064	2050	6889	3364420	85795
2006	66755	7120426	2039	6889	3364515	85442
2007	66038	7133608	1918	6893	3352462	85147
2008	65167	7157281	2304	6894	3329530	84890
2009	65398	7178806	2561	6898	3307656	84747
2010	74245	7204335	2664	6898	3273439	84485
2011	77592	7230744	2338	6901	3244033	84458
2012	80805	7251330	2188	6902	3220385	84456
2013	91938	7250752	2260	6902	3209473	84741
2014	93901	7252606	2693	6902	3205272	84692
2015	99689	7261931	3350	6903	3189439	84754
2016	107767	7267362	3817	6903	3175185	85032
2017	102114	7255293	2959	6905	3178854	99941
2018	94742	7332308	2765	6911	3124827	84513
2019	87039	7389746	2365	6911	3075704	84301
2020	93403	7371140	1905	6917	3088392	84309

Table A2. Spectral Bands of the MODIS NDVI products used in this paper.

Band	Units	Bit type	Fill	Valid Range	Scale
Band 1 Red	Reflectance	16-bit signed integer	-1000	0, 10000	0.0001

Band 2 Near-infrared	Reflectance	16-bit signed integer	-1000	0, 10000	0.0001
Band 3 Blue	Reflectance	16-bit signed integer	-1000	0, 10000	0.0001
Band 4 Mid-infrared	Reflectance	16-bit signed integer	-1000	0, 10000	0.0001

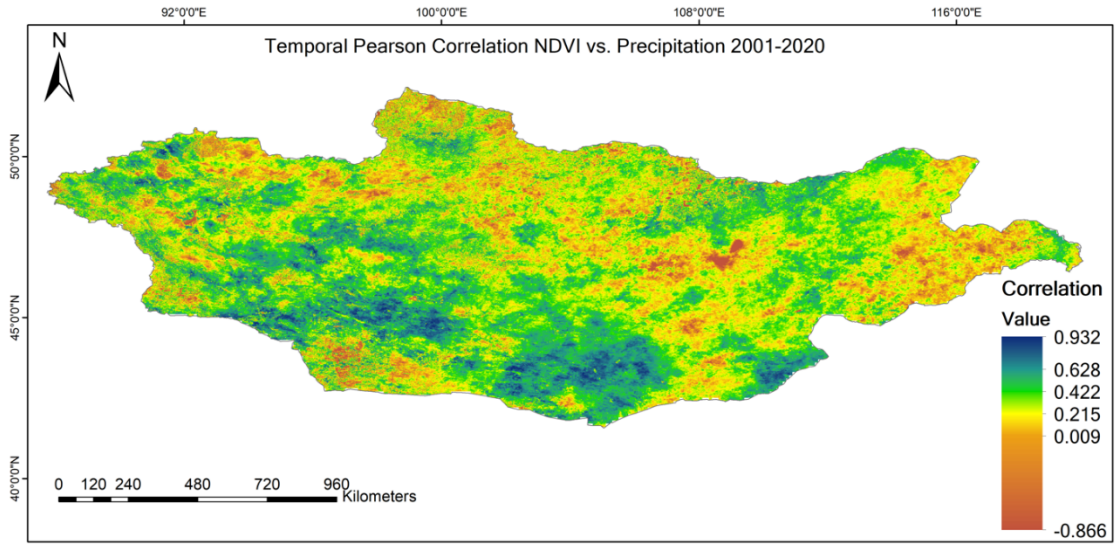

Figure A2. The Temporal Pearson Coefficients between NDVI and Precipitation from 2001 to 2020 in float point format.